THE JOURNAL OF BIOLOGICAL CHEMISTRY
Vol. 277, No. 44, Issue of November 1, pp. 41857–41864, 2002

Printed in U.S.A.

Crystal Structure of the 47-kDa Lipoprotein of *Treponema pallidum* Reveals a Novel Penicillin-binding Protein*

Received for publication, July 23, 2002, and in revised form, August 7, 2002
Published, JBC Papers in Press, August 24, 2002, DOI 10.1074/jbc.M207402200

Ranjit K. Deka‡, Mischa Machius§, Michael V. Norgard‡¶, and Diana R. Tomchick§

From the Departments of ‡Microbiology and §Biochemistry, University of Texas Southwestern Medical Center, Dallas, Texas 75390

Syphilis is a complex sexually transmitted disease caused by the spirochetal bacterium *Treponema pallidum*. *T. pallidum* has remained exquisitely sensitive to penicillin, but the mode of action and lethal targets for β-lactams are still unknown. We previously identified the *T. pallidum* 47-kDa lipoprotein (Tp47) as a penicillin-binding protein (PBP). Tp47 contains three hypothetical consensus motifs (SVTK, TEN, and KTG) that typically form the active center of other PBPs. Yet, in this study, mutations of key amino acids within these motifs failed to abolish the penicillin binding activity of Tp47. The crystal structure of Tp47 at a resolution of 1.95 Å revealed a fold different from any other known PBP; Tp47 is predominantly β-sheet, in contrast to the α/β-fold common to other PBPs. It comprises four distinct domains: two complex β-sheet-containing N-terminal domains and two C-terminal domains that adopt immunoglobulin-like folds. The three hypothetical PBP signature motifs do not come together to form a typical PBP active site. Furthermore, Tp47 is unusual in that it displays β-lactamase activity (k_{cat} for penicillin = 271 ± 6 s^{-1}), a feature that hindered attempts to identify the active site in Tp47 by co-crystallization and mass spectrometric techniques. Taken together, Tp47 does not fit the classical structural and mechanistic paradigms for PBPs, and thus Tp47 appears to represent a new class of PBP.

Syphilis is a chronic, complex sexually transmitted disease of humans caused by the spirochetal bacterium *Treponema pallidum*. Humans are the only known reservoir for *T. pallidum*, and although syphilis is one of the oldest recognized sexually transmitted diseases, a major impediment to research on *T. pallidum* continues to be the inability to cultivate the organism *in vitro*. Consequently, despite decades of intensive efforts, many features of *T. pallidum* ultrastructure, physiology, and membrane biology remain obscure (1).

T. pallidum is exquisitely sensitive to penicillin, which continues to be the drug of choice for syphilotherapy. Penicillin and other β-lactams are bactericidal via their ability to inhibit cytoplasmic membrane-bound enzymes (penicillin-binding proteins (PBPs))[1] involved in peptidoglycan biosynthesis (2). Generally, bacteria contain several PBPs that are classified within two categories (high molecular weight or low molecular weight) (3, 4). In *Escherichia coli*, the high molecular weight PBPs tend to be bifunctional (transglycosylase/transpeptidase activities) and are the lethal targets of β-lactams (5). The low molecular weight PBPs can be either monofunctional DD-carboxypeptidases, bifunctional DD-carboxypeptidases/DD-endopeptidases, or monofunctional DD-endopeptidase (6). In *T. pallidum*, the lethal targets for β-lactams are not known. However, two previous studies in which *T. pallidum* was incubated *in vitro* with radiolabeled β-lactams implicated polypeptides of 94, 80, 63, 58, 47, and 38 kDa (7) or 180, 89, 80, 68, 61, 41, and 38 kDa (8) as PBPs. As a follow-up to an earlier study by us (7), we have shown that the major 47-kDa membrane lipoprotein of *T. pallidum* (Tp47) is a PBP. More recent genome information (9) has suggested that *T. pallidum* encodes at least three theoretical PBPs of molecular masses of 71 (TP0500, PBP-1; TP0760, PBP-3) and 98 (TP0705; PBP-2) kDa, but direct biochemical evidence for these proteins as PBPs are lacking. An additional protein putatively has been assigned as a serine-type DD-carboxypeptidase (53-kDa, TP0800), and another as a DD-carboxypeptidase (29-kDa, TP0221). No β-lactamases have been predicted to be present in *T. pallidum* (9).

The notion that Tp47 is a PBP has been paradoxical. First, Tp47 has no homologies with any other bacterial or eukaryotic proteins. Second, conventional PBPs contain three conserved motifs, S*XX*K, S(Y)*X*N, and KT(S)G, which comprise the active site for the covalent binding of β-lactams (10–12). The serine of the S*XX*K motif is important for nucleophilic attack on the β-lactam ring. Tp47 contains three such appropriately spaced hypothetical motifs (SVTK, TEN, KTG) (13). However, preliminary experiments replacing Ser in the SVTK motif of Tp47 with Gly, Ala, Cys, or Thr all yielded mutant enzymes that still bound β-lactam comparable with wild-type Tp47 (14). Finally, lipidation of PBPs also is uncommon (15).

The numerous incongruities surrounding Tp47 as a PBP prompted the current biochemical and biophysical study. Specifically, it was envisioned that precise structural information derived from x-ray crystallography could provide strategic information to guide future biochemical studies on the enzymatic activity of Tp47. In this study, it was found that Tp47 has a crystal structure unique to any other known PBP, and thus it appears to represent an entirely new class of PBP.

* This work was supported by Grant AI-16692 from the NIAID, National Institutes of Health, and by Grant I-0940 from the Robert A. Welch Foundation. Use of the Argonne National Laboratory Structural Biology Center beamline at the Advanced Photon Source was supported by the United States Department of Energy, Office of Biological and Environmental Research, under Contract W-31-109-ENG-38. The costs of publication of this article were defrayed in part by the payment of page charges. This article must therefore be hereby marked "*advertisement*" in accordance with 18 U.S.C. Section 1734 solely to indicate this fact.

¶ To whom correspondence should be addressed: Dept. of Microbiology, University of Texas Southwestern Medical Center, 6000 Harry Hines Blvd., Dallas, TX 75390. Tel.: 214-648-5900; Fax: 214-648-5905; E-mail: michael.norgard@utsouthwestern.edu.

[1] The abbreviations used are: PBP, penicillin-binding proteins; Dig-Amp, digoxigenin-labeled ampicillin; MALDI-TOF, matrix-assisted laser desorption ionization time-of-flight; ESI-MS, electrospray ionization-mass spectrometry; NAM, *N*-acetylmuramic acid.

EXPERIMENTAL PROCEDURES

Construction of Wild-type and Variant Tp47-Streptavidin Fusion Proteins—The post-translationally modified N-terminal cysteine of native Tp47 was designated as amino acid 1 (16). To ensure production in *E. coli* of a nonlipidated version of Tp47, a DNA fragment encoding amino acids 2–415 (residue 415 is the last amino acid before the first TAG termination codon in *tp47*) (16) was amplified by PCR using *T. pallidum* genomic DNA (17) as template. The PCR primers were 5′-tcc**CCGCGG**CTCGTCTCATCATGAGACGCA-3′ and 5′-catg**CCATGG**TTACTACTGGGCCACTACCTCGCA-3′. The forward primer contained both a tcc overhang and a *Sac*II site (bold); the reverse primer contained a catg overhang, a *Nco*I site (bold), and two contiguous stop codons (TTA, CTA). PCR amplification was performed using Vent DNA polymerase (New England Biolabs). Amplified fragments were cleaved with *Sac*II and *Nco*I and cloned directionally into *Sac*II- and *Nco*I-cleaved pASK-IBA7 vector (Sigma). This construct was designated as wild type, and was verified by DNA sequencing and then transformed into *E. coli* DH5α.

Site-directed mutagenesis of *tp47* was carried out by a PCR-based method, using two complementary mutation-harboring oligonucleotides for each mutant and the QuikChange site-directed mutagenesis kit (Stratagene). Five different mutant genes were constructed; four encoded proteins with single amino acid substitutions and one contained a double substitution. The mutant proteins expressed were designated as Tp47S100G, Tp47S100C, Tp47K287Q, Tp47C296A, and Tp47H5S/H9S, based on the amino acid positions involved. Finally, a fusion construct in which C-terminal residues 329–415 were deleted (corresponding to Domain D; see crystal structure Fig. 2 (Tp47ΔD)) also was constructed by PCR subcloning as described above, except that the reverse primer was 5′-catg**CCATGG**TTACTAATCAGCAACTACGTCC-3′. All resulting mutants were sequenced to verify the specific mutation(s) intended. Mutant *tp47* genes were expressed in *E. coli*, and the cognate proteins were purified as described below for wild-type Tp47. SDS-PAGE analysis revealed that the mutants expressed quantities of proteins comparable with wild-type Tp47, suggesting that none of them was unstable (data not shown).

Expression and Purification of Tp47—*E. coli* DH5α containing the respective cloned *tp47* gene fusion was grown at 37 °C in LB medium containing 100 μg of ampicillin per ml; when the A_{600} of the culture reached 0.6, the culture was shifted to 30 °C and expression of the Tp47-streptavidin fusion protein was induced (via a *tetA* promoter) by the addition of 200 μg/liter of anhydrotetracycline. After 3 h, cells were harvested by centrifugation and solubilized by B-PER II (Pierce). After centrifugation at 15,000 rpm for 20 min (4 °C) to remove cellular debris, the supernatant was loaded onto a StrepTactin-Sepharose column. The fusion protein was then purified according to the Strep-tag II protein expression and purification system manual (Sigma). The yield of purified proteins tended to be about 25 mg/liter of bacterial culture. Purified protein was subjected to buffer exchange with buffer A (20 mM Hepes buffer, pH 7.4, 20 mM NaCl) using a PD-10 column (Amersham Biosciences). The protein was then concentrated to about 15 mg/ml using a Centricon YM-10 device (Amicon). Protein purity was analyzed by SDS-PAGE (18) and by electrospray ionization-mass spectrometry (ESI-MS). The concentration of purified protein was estimated spectrophotometrically using a calculated extinction coefficient of $\epsilon_{280} = 54{,}050\ \text{M}^{-1}\ \text{cm}^{-1}$ (19).

β-Lactam Binding to Tp47—Binding of digoxigenin-labeled ampicillin (Dig-Amp) to Tp47 was determined by a chemiluminescent detection method (13, 20); the use of Dig-Amp circumvents problems associated with utilizing radiometric methods for assaying β-lactam binding (20). β-Lactam binding to Tp47 also was examined by ESI-MS; in these experiments, a typical 100-μl reaction mixture contained 100 μg of protein, 2 mM $ZnCl_2$, and 2 mM β-lactam (in buffer A) and was incubated at 37 °C for various times. The reaction was terminated by the addition of 30 μl of 5% formic acid. Excess β-lactam was removed by a Microcon YM-30 device (Amicon), and samples were recovered in 1% formic acid for ESI-MS analysis (21). The peak heights of free and acylated Tp47 were measured from the ESI-MS spectra and the percentage of Tp47 acylation was calculated using the equation: % acylation = [acylated Tp47/(acylated Tp47 + free Tp47)] × 100 (22). In an attempt to identify the Tp47 amino acid involved in penicillin binding, liganded sample was digested with trypsin in 100 mM ammonium bicarbonate (pH 7.8, 37 °C); after digestion for various times, samples were subjected to MALDI-TOF MS (23).

Kinetic Analysis of β-Lactamase Activity—The hydrolytic activity of Tp47 on various β-lactams was assessed at 37 °C in buffer A using a Shimadzu UV-1601PC UV-visible spectrophotometer equipped with a thermostated multicell transport system. The molar absorption coefficients used were as follows: penicillin G, $\Delta\epsilon_{235} = -775\ \text{M}^{-1}\ \text{cm}^{-1}$; ampicillin, $\Delta\epsilon_{235} = -820\ \text{M}^{-1}\ \text{cm}^{-1}$; nitrocefin, $\Delta\epsilon_{486} = 16{,}000\ \text{M}^{-1}\ \text{cm}^{-1}$. β-Lactam solutions were freshly prepared in buffer A. Initial rates were determined from the first 5–10% of the reactions at various substrate concentrations. K_m and V_{max} values were determined by fitting all data to the Lineweaver-Burk equation using the program UV Probe (Shimadzu).

Tazobactam inhibition of the hydrolytic activity of Tp47 was performed with penicillin as a competitor substrate in buffer A. Tazobactam at various concentrations was preincubated with Tp47 for 5 min at 37 °C before the addition of penicillin. Steady-state rates during the course of penicillin hydrolysis were used to calculate the remaining activity. The inhibition constant (K_i) was deduced from Dixon plots using the UV Probe software.

Protein Crystallization and Data Collection—Wild-type Tp47 described above did not yield crystals in preliminary screening experiments. However, one of the variant versions of Tp47, in which His-5 and His-9 were replaced with Ser (Tp47H5/H9S; Fig. 1), crystallized readily and thus was designated as crystallizable Tp47 (cTp47). Of particular importance, cTp47 retained PBP activity comparable with the wild-type (Fig. 1). cTp47 was crystallized by the hanging-drop vapor diffusion method (24) using 24-well Linbro plates (Hampton Research) at room temperature. Sparse matrix crystallization kits (Hampton Research) were used to screen preliminary crystallization conditions. Crystals of average dimension of 50 μm appeared within 3–4 weeks. Further growth of the crystals was hindered because of phase separation/oil formation, and these crystals diffracted poorly to a Bragg spacing (d_{min}) of 6 Å. Crystallization optimization using dextran sulfate eliminated the phase separation and yielded substantially larger crystals (about 500 μm) within 2–4 days that diffracted to better than a d_{min} of 3 Å. Crystals were routinely obtained with drops containing 5 μl of protein solution (about 15 mg/ml in buffer A), and 5 μl of 32% (w/v) PEG 4000 in 100 mM sodium citrate, pH 5.6, 200 mM ammonium acetate, 3% (w/v) dextran sulfate 8000 (Sigma), and ±100 μM $ZnCl_2$, equilibrated against 500 μl of the latter solution at room temperature. Prior to data collection, crystals were transferred sequentially for 5 min to each of 5, 10, and 15% (v/v) glycerol-enriched reservoir solution for cryogenic conditioning. Diffraction data were collected at 100 K using a Rigaku RU300 rotating copper anode x-ray generator and *R*-axis IV image plate detector (Molecular Structures Corp., The Woodlands, TX). The diffraction data were indexed, integrated, and scaled in the HKL2000 program package (25).

The cTp47 crystals were found to exhibit the symmetry of space group $P3_221$ with unit cell dimensions of $a = b = 129.1$ Å, $c = 151.5$ Å. The crystals contained two molecules per asymmetric unit. The crystal structure of cTp47 was determined by single wavelength anomalous dispersion using a xenon derivative. The xenon derivative of a cTp47 crystal was prepared by exposing a preconditioned native crystal (in glycerol-enriched reservoir solution) in a xenon chamber (kindly provided by Zhenming Wang) at 400 p.s.i. for 15 min at room temperature. The chamber was then depressurized and the crystal flash-cooled in liquid propane within 15 s. Diffraction data to a d_{min} of 2.28 Å were recorded. The data were reduced with the program package HKL2000. Xenon sites were identified and refined to 3.0 Å within the program package CNS (version 1.0) (26), resulting in an overall figure of merit of 0.35. The phases were further improved by density modification in CNS including histogram matching, solvent flipping, and phase extension to a d_{min} of 2.28 Å, resulting in a final figure of merit of 0.95 (Table I). After the structure was solved, a synchrotron data set on a xenon-derivatized cTp47 crystal was collected to a d_{min} of 1.95 Å at the Structural Biology 19-ID beamline at the Advanced Photon Source (Argonne National Laboratory, Argonne, IL). Data collection and single wavelength anomalous dispersion phasing statistics are provided in Table I.

Model Building and Structure Refinement—Model building was performed automatically (arp_warp 5.0) (27) and manually with the program O (28). Structure refinement using the synchrotron data set was carried out within CNS employing cycles of simulated annealing, conjugate gradient minimization, and calculation of individual atomic displacement parameters. An overall anisotropic atomic displacement parameter and bulk solvent correction were used throughout the refinement procedure. Water molecules were added where stereochemically reasonable after the protein part of the model was complete. Inspection of the $F_{obs} - F_{calc}$ difference density map revealed a large volume of positive difference density extending across the noncrystallographic 2-fold axis, and located in the positively charged cleft between domains B and C of each monomer. This density was modeled as a

TABLE I
Data collection and refinement statistics
Data collection values are as defined in the program SCALEPACK (25). Model refinement values are as defined in the program CNS (26).

Data set	Laboratory source	Synchrotron
A. Data Collection		
Wavelength	Cu-K_α	0.97938 Å
Space group	$P3_221$	$P3_221$
Cell dimensions	a = 129.1 Å, c = 151.5 Å	a = 128.9 Å, c = 151.2 Å
Data range (Å)	30.4–2.17	28.2–1.95
No. of measurements	521,495	478,972
No. of independent reflections	139,645[a]	105,601
R_{merge} (%)[b]		
Overall	4.6	5.8
Last shell	53.0 (2.20–2.17 Å)	70.2 (2.02–1.95 Å)
Data completeness (%)		
Overall	93.1	99.8
Last shell	82.3	100
$I/(\sigma)I$		
Overall	22.3	21.4
Last shell	2.0	1.9
R. refinement		
No. of reflections used in refinement		
Working set		94,665 (35.0–1.95 Å)
Test set		5,036
No. of non-H protein atoms		6,356
No. of Xe atoms		5
No. of polysaccharide atoms		39
No. of water molecules		407
R_{work} (%)		21.2
R_{free} (%)		23.5
R.m.s.d. in bond lengths (Å)		0.010
R.m.s.d. in bond angles (°)		1.45
Mean B value (Å^2)		
Main chain		41.6
Side chain		44.5
Xenon atoms		46.7
Polysaccharide atoms		62.4
Water molecules		41.3
σ_A-Coordinate error (Å)		0.22
Missing residues		Molecule A: 2–6, 35–43, 415 Molecule B: 2–6, 35–39, 414–415
No. of alternate conformations		14

[a] This data set was scaled with Bijvoet pairs unmerged.
[b] $R_{merge} = 100\sum_h \sum_i |I_{h,i} - \langle I_h \rangle| / \sum_h \sum_i I_{h,i}$, where the outer sum ($h$) is over the unique reflections and the inner sum (i) is over the set of independent observations of each unique reflection.

dextran sulfate polysaccharide with an α1→6 linkage and two sulfate groups (on O-2 and O-3) per glucose. The final model contains residues 7 to 34 and 44 to 414 of molecule A, and residues 7 to 34 and 40 to 413 of molecule B, 14 residues with alternate conformations, five xenon atoms, two complete and two partial sugar moieties of a dextran sulfate polysaccharide, and 407 water molecules. Residues 2 to 6, 35 to 43, and 415 in molecule A, and residues 2 to 6, 35 to 39, and 414 to 415 in molecule B were disordered in the crystal structure and could not be traced in the electron density. The final R_{free} value is 23.5% and the R_{work} value is 21.2% (Table I).

Analytical Ultracentrifugation—Sedimentation equilibrium studies were performed in a Beckman XL-1 Optima analytical ultracentrifuge at 4 °C. Tp47 samples corresponding to absorbancies of 0.1, 0.2, and 0.4 at 280 nm in buffer A were used. Samples were centrifuged at 14,000 × g to remove aggregates prior to loading. Experiments were conducted at a rotor speed of 13,000 and 18,000 rpm and the radial scans at 280 nm were recorded until equilibrium was reached. The sedimentation equilibrium data were analyzed using the supplied software.

RESULTS AND DISCUSSION

Expression and Purification of Tp47—Bacterial lipoproteins are membrane proteins by virtue of their three long-chain fatty acids (post-translationally added to an N-terminal cysteine) that serve solely as membrane insertion anchors (29). As such, the long-chain fatty acids do not contribute to the conformation of the protein. The proteins, in the absence of their acyl chains, thus tend to be water soluble (consistent with the polypeptides protruding into the periplasm or extracellular environment). A cloning strategy therefore was implemented in which the leader sequence and N-terminal cysteine codon of *tp47* were deleted, ultimately to yield a nonlipidated, water soluble version of Tp47. Finally, soluble Tp47 and its variants were created as fusion proteins with an N-terminal streptavidin tag, which is only 18 amino acids long; the streptavidin tag thus should have minimal, if any, conformational influence on Tp47. This contention was corroborated by the findings that the fusion proteins performed as predicted in PBP assays (see below).

Properties of Mutant Tp47 Enzymes—Ser-100 of a putative SVTK tetrad in Tp47 (13) was altered to cysteine (Tp47S100C); this mutation did not abolish Dig-Amp binding (Fig. 1) or penicillin binding to Tp47 (ESI-MS data not shown). Similarly, conversion of Ser-100 to glycine did not abrogate the binding of penicillin to Tp47, as assessed by ESI-MS (not shown). Thus, as initially proposed (14), it appears that Tp47 does not employ an active-site serine to serve as a nucleophile and subsequent covalent attachment site for β-lactams. This is in sharp contrast to what has been observed for other classical PBPs (30, 31). That a mutation of the presumptive active site serine had no influence on the PBP activity of Tp47 provided the first compelling evidence that Tp47 might be dissimilar from other conventional, serine-type PBPs.

The KTG triad also forms a key component of the active site cleft and is highly conserved within PBPs (10–12). However, if Tp47 is not a serine-type PBP, it was postulated that the KTG motif in Tp47 may be coincidental, or may function in some other unknown manner. For example, the positive charge on the Lys might interact with the carboxylate group of the D-Ala-

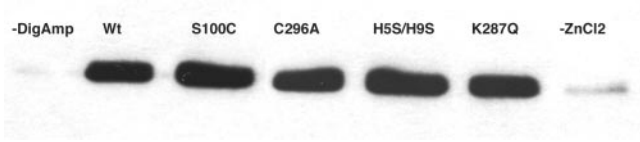

FIG. 1. **Binding of Dig-Amp to wild-type (*Wt*) and mutant variants of Tp47.** Recombinant versions of Tp47 incubated with Dig-Amp were separated by SDS-PAGE, electrotransferred to nylon membrane, and developed by chemiluminescence (13, 20). Dig-Amp binding was assessed in the presence of $ZnCl_2$ except where noted ($-ZnCl_2$). *−Dig-Amp*, wild-type Tp47 without Dig-Amp treatment.

D-Ala, and hence the carboxylate group of penicillin (30, 32). However, when Lys-287 of the KTG triad in Tp47 was mutated to Gln (Tp47K287Q), the mutant protein retained its penicillin binding activity (Fig. 1). Inasmuch as the mutation of Lys in the KTG motifs of other PBPs typically adversely impacts PBP activity (30), our results further underscore the atypical character of Tp47.

cTp47 Structure—Findings that Tp47 seemed not to rely on either an active site serine (of SVTK) nucleophile or a KTG motif for PBP activity were anomalous. This prompted a structural approach to gain further insights into the structure-function relationships for Tp47 as perhaps a novel PBP. Initially, crystal growth of cTp47 was hampered by the occurrence of phase separation, and the resulting crystals were small and diffracted poorly to a Bragg spacing (d_{min}) of 6 Å. Phase separation could be overcome by the addition of dextran sulfate, resulting in larger crystals (up to 500 μm in the largest dimension) that diffracted to a d_{min} of 3 Å. These crystals exhibited the symmetry of space group $P3_221$, with two molecules per asymmetric unit. The crystal structure of cTp47 was determined via the single wavelength anomalous dispersion technique using a xenon derivative. Derivatization with xenon not only provided phase information, but also increased the diffraction limit of the cTp47 crystals to a d_{min} of 1.95 Å using synchrotron radiation.

The crystal structure of cTp47 revealed four distinct domains arranged to give the molecule a crab-like appearance (Fig. 2). The first domain (domain A; residues 7 to 34 and 156 to 204) is mainly composed of β-strands and is sequentially non-contiguous. The core of this domain is formed by a strand-helix-strand motif (Aβ2-Aα3-Aβ3) (Fig. 3) in a right-handed superhelical arrangement. Adjacent to Aβ2 is a β-hairpin (strands Aβ4 and Aβ5) whose tip interacts with the helix to create a barrel-like structure. The N terminus of cTp47 forms a β-strand (Aβ1) that inserts between Aβ2 and Aβ3 to complete a five-stranded, highly twisted, mixed β-sheet (order 3, 1, 2, 4, 5). A helix-loop-helix motif (Aα1 and Aα2) next to the β-hairpin completes domain A and connects to the adjacent domain B. A structural comparison of this domain using the program DALI (33) did not reveal any similarity with proteins in the Protein Data Bank (highest Z-score of 1.7). The largest recognizable structural motif within this domain is generated by strand Aβ1, helix Aα3, and strand Aβ3 that forms an anti-parallel two-stranded β-sheet with an opposing helix. This motif also has been observed in the *Lactobacillus casei* Hpr kinase (Protein Data Bank code 1jb1).

Domain B (residues 44 to 155) contains 10 β-strands and a single α-helix (Figs. 2 and 3). Its main structural feature is a central four-stranded, anti-parallel β-sheet (strands Bβ1, Bβ10, Bβ2, and Bβ5). This sheet is opposed by an α-helix (Bα1) resulting in an arrangement that resembles a right hand, with the strands being the fingers (strand Bβ1 is the index finger) and the helix as the thumb. The backside of the sheet forms a flat outer surface. At the N and C termini of strand Bβ5 are two large β-hairpins (strands Bβ3/Bβ4 and Bβ8/Bβ9) that are oriented perpendicular to the central sheet. These hairpins, together with large connecting loops and a third β-hairpin (strands Bβ5/Bβ6) in between them, form a second flat outer surface. The central motif consists of strands Bβ1, Bβ10, and Bβ3, and helix Bα1, which is typical of cysteine proteases (34). In fact, the topology of domain B in cTp47, except for the hairpin formed by strands Bβ3 and Bβ4, is conserved in the cysteine protease staphopain from *Staphylococcus aureus* (Protein Data Bank code 1cv8). Yet, Tp47 does not appear to be a cysteine protease as a cysteine is not present in a region equivalent to the active site in cysteine proteases. Furthermore, mutation of the sole Cys (Cys-296, which is buried in the hydrophobic core of domain C) to alanine had no effect on PBP activity (Fig. 1), thereby ruling out involvement of this residue in catalysis.

Domain C (residues 205 to 332) is the largest domain (Fig. 2). It is mainly characterized by an immunoglobulin fold with two opposing β-sheets that form the typical barrel-like structure. In contrast to the classical immunoglobulin fold, however, domain C of cTp47 has an additional β-strand inserted after strand 3. Also, the strands are connected by rather large loops. Helices are inserted between strands 2 and 3 and between strands 4 and 5.

Domain D (residues 333 to 414) also features an immunoglobulin fold. In contrast to domain C, it contains only the characteristic seven-stranded barrel and short loops. As in domain C, a single α-helical turn is inserted between strands 2 and 3.

Dimer Formation—In our crystals of cTp47, a dimer was formed between two neighboring molecules (Fig. 4). Domains B and D act as the pincers on a crab that make contact with the pincers of the opposing molecule. The monomer-monomer interface has an area of about 1,830 Å^2 and features a series of polar and hydrophobic interactions as well as six ionic interactions. This finding prompted further assessment of Tp47 dimer formation in free solution by analytical ultracentrifugation. The sedimentation equilibrium data profile produced by analytical ultracentrifugation fit well to a model comprising a single species of molecular mass of 46,178 Da (not shown), consistent with the monomeric mass determined by SDS-PAGE and ESI-MS, supporting the observation that Tp47 displays monomeric characters in free solution. Consequently, Tp47 dimer formation observed within the crystal structure could be a result of crystallization, with the high salt concentration driving a nonspecific association of the hydrophobic surfaces, as has been noted for other proteins undergoing crystal packing (35, 36). In fact, when domain D (which is not required for PBP activity) is removed from the buried surface area calculation, only ~850 Å^2 surface area is buried at the monomer-monomer interface. This is a value found at the upper limit of buried surface area for nonspecific crystal contacts (37).

Domain Interfaces—The first three domains in cTp47 interact with each other through intimate domain-domain interfaces. Domain A contacts domain B through its N-terminal segment that contains β-strand Aβ1 and the helix-loop-helix motif, establishing interactions with the loop regions before the first β-strand (Bβ1) and after the last β-strand (Bβ10) in domain B. The first linking region between these domains (residues 34 and 44) is disordered in the crystal structure. Domain A also interacts tightly with domain C, involving mainly side chains in helix Aα2 and the loop region between β-strands Aβ3 and Aβ4 in domain A and β-strands Cβ3β and Cβ6 as well as the loop region between strands Cβ6 and Cβ7.

Domain B interacts with domain C via a surface that has a slightly concave, goblet-like shape. The long loops proximal to strand Bβ1 and between strands Bβ5 and Bβ6 form the sides, and helix Bα1 forms the bottom of the goblet. Residues in these

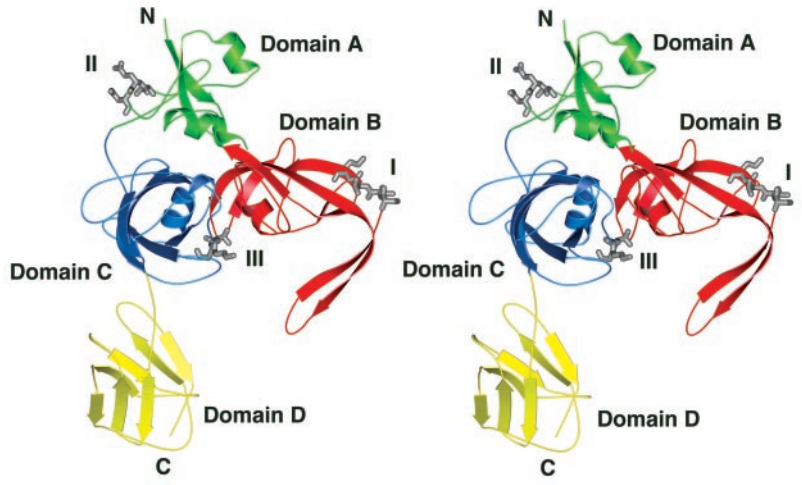

FIG. 2. **Stereoview of the cTp47 monomer.** Domains A–D are drawn in different colors to highlight the domain boundaries. The residues of the hypothetical PBP sequence motifs are labeled I (^{100}SVTK), II (^{183}TEN), and III (^{287}KTG) (*gray sticks*). Figs. 2, 4, and 5 were prepared with the programs BobScript (51), POV-Ray (www.povray.org), and GLR (L. Esser, personal communication).

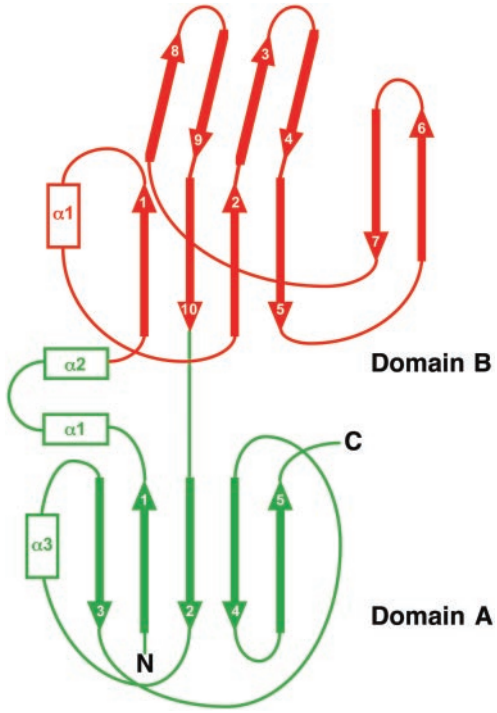

FIG. 3. **Topology diagram of domain A (*green*) and domain B (*red*) of cTp47.** Strands are depicted as *arrows*, and helices are shown as *rectangular boxes*. Strands and helices are numbered sequentially for each domain. The N and C termini of domain A are shown.

regions establish a number of polar and hydrophobic interactions with residues at the surface of domain C, which includes strands Cβ3, Cβ3β, and Cβ4, the loop region between strands Cβ5 and Cβ6, and helix Cα1. Adjacent to this interaction surface is a deep cleft located between the β-hairpin Bβ3/Bβ4 and the rest of domain B. The tip of this hairpin, as well as the portion of this surface that is not involved in interactions with domain C, are highly positively charged containing five arginines, two histidines, and two lysines.

In contrast to domains A, B, and C, domain D is rather isolated. It interacts only with domain C via an ionic interaction between Arg-330 and Glu-404 in the linker region. Consequently, the relative disposition of domain D is expected to vary. Evidence for a larger degree of domain motion can be found in the higher average displacement factors for the atoms of domain D relative to the first three domains (38.8 *versus* 57.8 Å^2 for monomer A, 38.0 *versus* 67.4 Å^2 for monomer B).

Comparison of Tp47 with Other PBP Structures—The three-dimensional structure of a conventional PBP typically is comprised of two structural domains, one of which is predominantly α and another that is α/β (38) (Fig. 5). The active site is positioned between these two major domains, at the edge of the central β-sheet of the α/β domain. The three signature sequence motifs of classical PBPs that putatively were present in Tp47 do not come together in three-dimensional space to form a typical active site. Given that Tp47 had no similarity to other known PBPs, it was hypothesized that it might represent a new family of PBPs. Consistent with this possibility, DALI did not identify Tp47 as a PBP, but rather had the highest structural homology (Z-score = 6.1) to non-PBPs.

Acylation and Deacylation of Tp47—The interaction between PBPs and β-lactams generally is described by the equation: $E + I \leftrightarrows E.I \rightarrow E\text{-}I \rightarrow E + P$, where E is the PBP enzyme, I is the β-lactam, $E.I$ is the Michaelis intermediate, E-I is the covalent acyl-enzyme complex, and P is the reaction product (*i.e.* cleaved, inactive β-lactam) (38). The formation of the enzymatically inactive (covalent) acyl-enzyme complex (E-I) is known as the acylation step. The covalent E-I complex results from the nucleophilic attack of the carbonyl carbon atom of the β-lactam ring by the hydroxyl group of the active site serine. The bactericidal efficiency of any β-lactam ultimately depends on the stability of the E-I complex. However, hydrolysis of the acyl-enzyme complex and release of the inactive β-lactam (P) occurs by a process known as deacylation; in the case of β-lactamases, deacylation is rapid. In former studies, Tp47 bound radiolabeled penicillin (7), and its binding to Dig-Amp subsequently was found to be stimulated by zinc ions (13). In the current study, upon incubation of purified Tp47 for 2 min with penicillin in the presence of zinc, two major peaks of 47,703 Da (free Tp47) and 48,036 Da (penicillin-bound Tp47) were detected by ESI-MS (not shown). The difference of 333 Da between the two molecular masses corresponded with the mass of penicillin (335 Da), indicating the formation of a covalent acyl-Tp47 complex bound predominantly in a 1:1 stoichiometry. Analogous results were obtained using ampicillin, carbenicillin, cefuroxime, and cephalosporin (not shown), indicating that recombinant Tp47 bound a number of β-lactams. In the absence of zinc, after 2 min of incubation, 5% of Tp47 became acylated, whereas, in the presence of zinc, 33% of Tp47 was acylated over the same interval (Table II), corroborating previous findings that the PBP activity of Tp47 appears to be stimulated by zinc (13). In the presence of zinc, acylation by penicillin was time-dependent, with maximal binding observed at 6 min (Table II). However, after 6 min, marked deacylation was evident, implying that Tp47 exhibits some intrinsic β-lactamase activity.

As shown in a previous study (13) and herein, zinc enhances

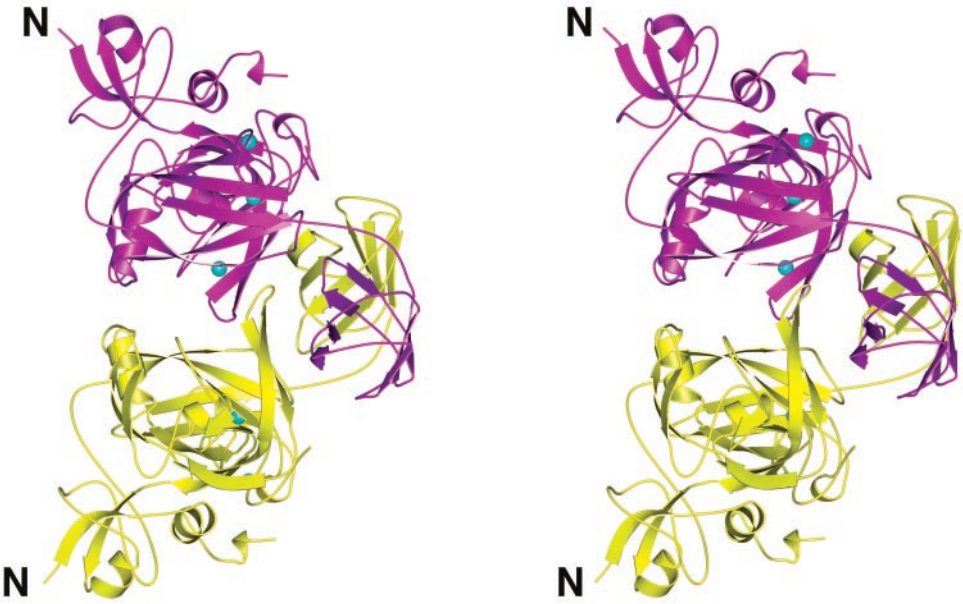

FIG. 4. **Stereoview of the cTp47 dimer.** The xenon atoms used in phasing the structure are represented as *cyan spheres*. The N termini of both monomers, which occur on the same face of the dimer, are oriented (as predicted) toward the cytoplasmic membrane surface.

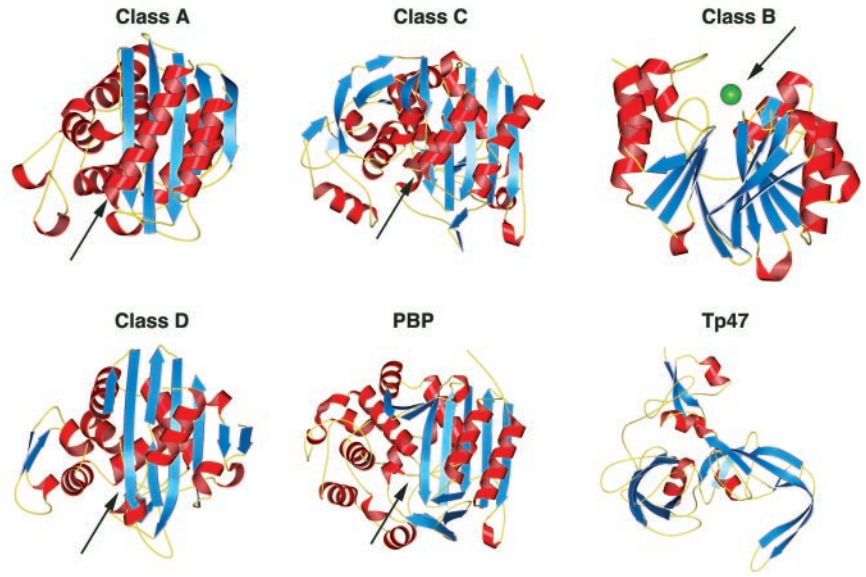

FIG. 5. **Comparison of the cTp47 structure to representative β-lactamases and PBPs.** Representative structures from the major classes of β-lactamases plus a D-Ala-D-Ala-peptidase/PBP are shown with *domains A–C* of Tp47 (domain D is not required for PBP/β-lactamase activity). *Black arrows* highlight the known active sites of the representative structures. The *green sphere* in the Class B structure represents a Zn^{2+} ion. The Class A structure is the TEM1 β-lactamase from *E. coli* (Protein Data Bank code 1btl), the Class B structure is the zinc metallolactamase from *Bacillus cereus* (Protein Data Bank code 1bmc), the Class C structure is the cephalosporinase from *Enterobacter cloacae* (Protein Data Bank code 2blt), the Class D structure is the Oxa-10 β-lactamase from *Pseudomonas aeruginosa* (Protein Data Bank code 1e3u), and the PBP structure is the D-Ala-D-Ala-peptidase/PBP from *P. aeruginosa* (Protein Data Bank code 1ceg).

TABLE II
Percent of Tp47 remaining acylated with penicillin at various times

Acylation reactions were carried out in either the presence (+) or absence (−) of 2 mM $ZnCl_2$.

Incubation time	% Acylation	
	$+Zn^{2+}$	$-Zn^{2+}$
min		
2	33	5
4	40	—[a]
6	50	—
10	35	5
20	28	—
30	27	ND[b]

[a] —, undetermined.
[b] ND, not detectable.

the binding of β-lactams to Tp47. This led to the initial idea that Tp47 was a zinc-dependent PBP (13). Two lines of evidence now challenge this view. First, we now show that rather than promoting acylation, zinc actually inhibits the deacylation of Tp47 (see below). Second, an *in vitro* carboxypeptidase assay using the synthetic depsipeptide substrate Sle (an analog of D-Ala-D-Ala) initially suggested that Sle was hydrolyzed by Tp47 in the presence of zinc, as indicated by an apparent increase in UV absorption at 254 nm (13). However, subsequent experiments have revealed that this apparent absorption increase is due, at least in part, to scattering caused by Tp47 aggregates that form in the presence of zinc (not shown). Hence, the initial contention that Tp47 might be a zinc-dependent carboxypeptidase (13) remains tenuous at this time.

Mass spectrometry has been employed for the identification of the penicillin-binding site in *Staphylococcus aureus* PBP 2a (21). Using a similar strategy, liganded Tp47 was digested with trypsin, and peptide fragments were assessed by MALDI-TOF MS. Attempts to identify a particular peptide fragment to which penicillin was bound were unsuccessful, suggesting that the acylated product was unstable during the procedure. One potential explanation for this was the intrinsic β-lactamase activity inferred in Table II.

TABLE III
Kinetic parameters for wild-type Tp47 hydrolytic activities using ampicillin, penicillin G, or nitrocefin at pH 7.4 (37 °C)

Substrate	k_{cat}	K_m	k_{cat}/K_m
	s^{-1}	μM	$s^{-1}\ \mu M^{-1}$
Ampicillin	187 ± 22	75 ± 7	2.49 ± 0.06
Penicillin G	271 ± 6	82 ± 3	3.31 ± 0.20
Nitrocefin	131 ± 28	94 ± 1	1.38 ± 0.28

Kinetic Parameters for Tp47 β-Lactamase Activities—Certain PBPs have intrinsic β-lactamase activity (30, 39). Kinetic analysis of β-lactam hydrolysis was used to assess whether the deacylation of Tp47 (Table II) was because of a similar intrinsic ability to hydrolyze β-lactams. The kinetic parameters of hydrolytic activities of Tp47 were determined for three β-lactams and are summarized in Table III. Tp47 exhibited an unexpectedly high level of β-lactam hydrolytic activity. Although the turnover rates (k_{cat}) for β-lactam hydrolysis by Tp47 were 10–20-fold lower than for typical β-lactamases (40), they are substantially higher than the β-lactamase activity of *E. coli* PBP5, which has an unusually high β-lactamase activity (k_{cat} = 0.07 s^{-1}) (39). On this basis, it could be conjectured that Tp47 is a β-lactamase. However, from a biological perspective, this notion is strongly inconsistent with the exquisite sensitivity of *T. pallidum* to β-lactams, particularly when the extraordinary abundance of Tp47 in *T. pallidum* is taken into account (41). Thus, the biological relevance of the putative Tp47 *in vitro* β-lactamase activity remains suspect, as it may be of little or no consequence to the biology of *T. pallidum in vivo* (*i.e.* during human infection). Interestingly, a higher level of penicillin binding to Tp47 was observed in the presence of zinc (Fig. 1 and Table II). As noted earlier, zinc also induces the aggregation of Tp47 (not shown), which appears as a suppression of *in vitro* β-lactamase activity. Taken together, it is tempting to speculate that the enhanced PBP activity of Tp47 has been observable, at least in part, by virtue of the inhibitory action of zinc on the intrinsic β-lactamase activity of Tp47. Finally, the *in vitro* hydrolytic activity of wild-type Tp47 was inhibited by tazobactam, an inhibitor of class A β-lactamases (42, 43), suggesting that competitive inhibition is active site directed. The apparent K_i value for hydrolysis of penicillin by wild-type Tp47 was 26.95 ± 0.35 nM.

Potential Active Site—Catalytic centers of PBPs have a conserved topology wherein three conserved motifs comprise the catalytic center (10, 11). The sequence of Tp47 has three such hypothetical signature motifs (13). However, mutations in the Ser of the putative SVTK motif and Lys of the KTG motif did not abrogate the PBP activity of Tp47 (Fig. 1). Furthermore, all three motifs of classical PBPs initially thought to be present in Tp47 are found in three different domains separated by distances greater than 30 Å (Fig. 2), supporting the contention that the three hypothetical motifs do not comprise the active site for β-lactam binding in Tp47. We thus conclude that Tp47 exhibits a unique mechanism for β-lactam binding. Further inspection of the structure therefore was undertaken to identify the active site. Emphasis was placed on searching for another reasonable PBP active site cleft, which might contain a Ser nucleophile spatially near another residue suitable for abstraction of a proton from the hydroxyl group of Ser (*e.g.* a positively charged amino acid such as Lys). Such efforts were not successful.

The predominance of hydrophobic residues and the immunoglobulin fold of domain D suggested that it might be utilized for protein-protein interaction(s) when in its native membrane setting within *T. pallidum*. In addition, the location, flexibility, and relative disposition of domain D suggests that it might not be involved in PBP and β-lactamase activities. In this regard, a domain D deletion mutant of Tp47 (Tp47ΔD) retained wild-type levels of both activities (not shown). Thus, it is reasonable to conclude that domain D has no catalytic role in the PBP activity of Tp47.

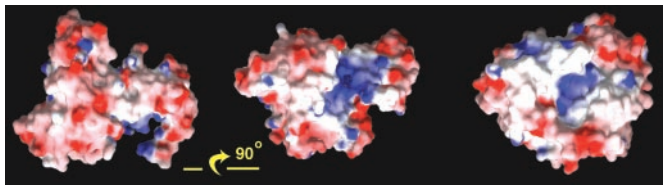

FIG. 6. **The cTp47 monomer has a positively charged cleft.** A surface representation of the electrostatic charge distribution for the Tp47 monomer (domains A–C) is shown at the *left* of the figure and is in the same orientation as in Fig. 2. The *central figure* was obtained via a rotation of 90° about the horizontal axis of the monomer. For comparison, the charge distribution for the active site cleft in the D-Ala-D-Ala-peptidase/PBP (Protein Data Bank code 1ceg) is shown at the *right* of the figure. The displayed surface potential varies approximately from −10 to 10 kT with acidic surfaces in *red* and basic in *blue*. The electrostatic surface potential was calculated and rendered in the program GRASP (52).

An analysis of the charge distribution on the surface of domains A–C of the Tp47 monomer is shown in Fig. 6. A positively charged cleft is found at the intersection of domains B and C, close to the domain B β-hairpin formed by strands Bβ3 and Bβ4. This cleft might function as a binding site for the carboxylate of D-Ala-D-Ala, and hence β-lactams. In the crystal structure, this cleft is found near the noncrystallographic 2-fold axis of the dimer. A dextran sulfate polysaccharide with an α1→6 linkage was modeled into the positive difference density found in this cleft. Approximately one-half of the electron density assigned to the polysaccharide is associated with each protein monomer, and the hydrogen-bonding pattern between the protein and each sulfated dextrose monosaccharide is similar. An attempt to model the polysaccharide backbone of naturally occurring peptidoglycan (repeating *N*-acetylmuramic acid (NAM) β1→4 linked to *N*-acetylglucosamine) into this density was not successful. An NAM monomer could be modeled into the density, but the β1→4 linkage of NAM-*N*-acetylglucosamine was inconsistent with the local 2-fold symmetry of the cleft. If Tp47 utilizes this cleft for the interaction of β1→4-linked peptidoglycan subunits, it appears that steric constraints dictate that the protein be in the monomeric state, as supported by our sedimentation equilibrium experiments. Whereas small crystals of cTp47 normally can be grown in the absence of dextran sulfate, crystallization with NAM or *N*-acetylglucosamine monosaccharides in place of dextran sulfate did not yield cTp47 crystals.

Further attempts to identify the active site of Tp47 by co-crystallization and/or soaking of crystals with β-lactams were unsuccessful, probably because of the deacylation activity noted earlier. A 3.8-Å data set was obtained from a co-crystallization and soak of cTp47 with the β-lactamase inhibitor tazobactam. The electron density map revealed changes in the positively charged cleft that may be because of a partial displacement of the dextran sulfate polysaccharide by the tazobactam, but an unambiguous fit of the inhibitor into this low resolution map was not possible.

Biological Significance and Implications—Tp47 was first noted in early molecular studies of *T. pallidum*, due largely to its abundance and profound immunogenicity (41). It thus initially was targeted for study as a potential syphilis serodiagnostic reagent (41, 44), and many newer generation serological tests for syphilis now include Tp47 as a principal, if not sole, antigenic component (45, 46). Tp47 initially also was thought to be an outer membrane protein (41). However, a more extensive

body of work, which has taken into account the previously unrecognized fragility of the unusual *T. pallidum* outer membrane (1, 47), later supported that Tp47 likely is a cytoplasmic membrane lipoprotein that, according to convention, would protrude into the periplasmic space (47, 48). This finding was more consistent with earlier studies that implicated it as a PBP (7, 13), inasmuch as PBPs reside at the cytoplasmic membrane (2). However, the precise role of Tp47 in the biosynthesis of *T. pallidum* peptidoglycan remains unclear. Although corroborative data are lacking, it is possible, implicated largely by its molecular mass, that Tp47 is a DD-carboxypeptidase. If so, the marked abundance of Tp47 would imply that it serves to limit the degree of cross-linking in the peptidoglycan of *T. pallidum*, thereby promoting the rather remarkable, highly flexuous motility pattern of the spirochete (49). Consistent with this view, other preliminary data have suggested that the expression of full-length, lipidated Tp47 in *E. coli* (13) reduces the degree of cross-linking in *E. coli* peptidoglycan.[2]

Despite both mutagenesis and x-ray crystallography data presented herein, identification of the putative active site of Tp47 for β-lactam binding remains unresolved. The three-dimensional structure of Tp47 has revealed a positively charged cleft that may bind monosaccharides and/or possibly tazobactam, and that cleft might function as an interaction site for the relevant carboxylate group of D-Ala-D-Ala (and β-lactams), but more conclusive evidence awaits further mutagenesis studies. Regardless, the combined data provide compelling evidence that Tp47 represents a new class of PBP. It also is not known to what extent this novel type of PBP might be found in other bacterial pathogens, but it is anticipated that the burgeoning genomics field will eventually shed additional light on this. Finally, it is noteworthy that although not sharing homology with Tp47, a completely α-helical cysteine-rich protein B of *Helicobacter pylori* recently was described as representing another new class of PBP (50). Although molecular modeling inferred that a site within the α-helical cysteine-rich protein B might bind to NAM, the crystal structure also did not definitively reveal the active site. Tp47 and the α-helical cysteine-rich protein B thus now seem to represent two examples of PBPs that do not satisfy classical PBP paradigms, the ramifications of which remain to be more fully explored.

Acknowledgments—We thank Taissia Popova and Martin Goldberg for assistance with mutant constructions, Sandra Hill for excellent technical assistance with crystal preparation and handling, Bikash Pramanik for mass spectrometry, John Buynak for supplying tazobactam, Joseph Albanesi for guidance with analytical ultracentrifugation, Zbyszek Otwinowski for assistance in processing the laboratory source xenon-derivatized data set, and Andrzej Joachimiak and the staff of the Structural Biology 19-ID beamline for expert aid in data collection.

REFERENCES

1. Radolf, J. D. (1995) *Mol. Microbiol.* **16,** 1067–1073
2. Ghuysen, J.-M. (1988) *Rev. Infect. Dis.* **10,** 726–732
3. Ghuysen, J.-M. (1991) *Annu. Rev. Microbiol.* **45,** 37–67
4. Massova, I., and Mobashery, S. (1998) *Antimicrob. Agents Chemother.* **42,** 1–17
5. Spratt, B. G. (1975) *Proc. Natl. Acad. Sci. U. S. A.* **72,** 2999–3003
6. Nelson, D. E., and Young, K. D. (2001) *J. Bacteriol.* **183,** 3055–3064
7. Radolf, J. D., Moomaw, C., Slaughter, C. A., and Norgard, M. V. (1989) *Infect. Immun.* **57,** 1248–1254
8. Cunningham, T. M., Miller, J. N., and Lovett, M. A. (1987) *J. Bacteriol.* **169,** 5298–5300
9. Fraser, C. M., Norris, S. J., Weinstock, G. M., White, O., Sutton, G. G., Dodson, R., Gwinn, M., Hickey, E. K., Clayton, R., Ketchum, K. A., Sodergren, E., Hardham, J. M., McLeod, M. P., Salzberg, S., Peterson, J., Khalak, H., Richardson, D., Howell, J. K., Chidambaram, M., Utterback, T., McDonald, L., Artiach, P., Bowman, C., Cotton, M. D., Fujii, C., Garland, S., Hatch, B., Horst, K., Roberts, K., Sandusky, M., Weidman, J., Smith, H. O., and Venter, J. C. (1998) *Science* **281,** 375–388
10. Spratt, B. G., and Cromie, K. D. (1988) *Rev. Infect. Dis.* **10,** 699–711
11. Goffin, C., and Ghuysen, J.-M. (1998) *Microbiol. Mol. Biol. Rev.* **62,** 1079–1093
12. Kelly, J. A., Kuzin, A. P., Charlier, P., and Fonze, E. (1998) *Cell. Mol. Life Sci.* **54,** 353–358
13. Weigel, L. M., Radolf, J. D., and Norgard, M. V. (1994) *Proc. Natl. Acad. Sci. U. S. A.* **91,** 11611–11615
14. Weigel, L. M. (1994) *Structure-function Relationships of the 47-kilodalton Major Membrane Lipoprotein of Treponema pallidum*, Ph.D. Dissertation, University of Texas Southwestern Graduate School of Biomedical Sciences
15. Hayashi, S., Hara, H., Suzuki, H., and Hirota, Y. (1988) *J. Bacteriol.* **170,** 5392–5395
16. Weigel, L. M., Brandt, M. E., and Norgard, M. V. (1992) *Infect. Immun.* **60,** 1568–1576
17. Norgard, M. V., and Miller, J. N. (1983) *Infect. Immun.* **42,** 435–445
18. Chamberlain, N. R., Brandt, M. E., Erwin, A. L., Radolf, J. D., and Norgard, M. V. (1989) *Infect. Immun.* **57,** 2872–2877
19. Gill, S. C., and von Hippel, P. H. (1989) *Anal. Biochem.* **182,** 319–326
20. Weigel, L. M., Belisle, J. T., Radolf, J. D., and Norgard, M. V. (1994) *Antimicrob. Agents Chemother.* **38,** 330–336
21. Sun, Y., Bauer, M. D., and Lu, W. (1998) *J. Mass Spectrom.* **33,** 1009–1016
22. Lu, W.-P., Sun, Y., Bauer, M. D., Paule, S., Koenigs, P. M., and Kraft, W. G. (1999) *Biochemistry* **38,** 6537–6546
23. van Oers, N. S. C., Tohlen, B., Malissen, B., Moomaw, C. R., Afendis, S., and Slaughter, C. A. (2000) *Nat. Immunol.* **1,** 322–328
24. McPherson, A. (1990) *Eur. J. Biochem.* **189,** 1–23
25. Otwinowski, Z., and Minor, W. (1997) *Methods Enzymol.* **276,** 307–326
26. Brunger, A. T., Adams, P. D., Clore, G. M., DeLano, W. L., Gros, P., Grosse-Kunstleve, R. W., Jiang, J. S., Kuszewski, J., Nilges, M., Pannu, N. S., Read, R. J., Rice, L. M., Simonson, T., and Warren, G. L. (1998) *Acta Crystallogr. Sect. D* **54**, 905–921
27. Perrakis, A., Morris, R. J., and Lamzin, V. S. (1996) *Nat. Struct. Biol.* **6,** 458–463
28. Jones, T. A., Zou, J. Y., Cowan, S. W., and Kjeldgaard, M. (1991) *Acta Crystallogr. Sect. A* **47**, 110–119
29. Hayashi, S., and Wu, H. C. (1990) *J. Bioenerg. Biomembr.* **22,** 451–471
30. van der Linden, M. P. G., de Haan, L., Dideberg, O., and Keck, W. (1994) *Biochem. J.* **303,** 357–362
31. Hadonou, A. M., Wilkin, J. M., Varetto, L., Joris, B., Lamotte-Brasseur, J., Klein, D., Duez, C., Ghuysen, J.-M., and Frere, J.-M. (1992) *Eur. J. Biochem.* **207,** 97–102
32. Malhotra, K. T., and Nicholas, R. A. (1992) *J. Biol. Chem.* **267,** 11386–11391
33. Holm, L., and Sander, C. (1993) *J. Mol. Biol.* **233,** 123–138
34. Turk, B., Turk, V., and Turk, D. (1997) *Biol. Chem.* **378,** 141–150
35. Ponsting, H., Henrick, K., and Thornton, J. M. (2000) *Proteins* **41,** 47–57
36. Kerfeld, C. A., Salmeen, A. E., and Yeates, T. O. (1998) *Biochemistry* **37,** 13911–13917
37. Janin, J., and Rodier, F. (1997) *Proteins* **23,** 580–587
38. Matagne, A., Lamotte-Brasseur, J., and Frere, J.-M. (1998) *Biochem. J.* **330,** 581–598
39. Davies, C., White, S. W., and Nicholas, R. A. (2001) *J. Biol. Chem.* **276,** 616–623
40. Kelly, J. A., Dideberg, O., Charlier, P., Wery, J. P., Libert, M., Moews, P. C., Knox, J. R., Duez, C., Fraipont, C., Joris, B., Dusart, J., Frere, J. M., and Ghuysen, J. M. (1986) *Science* **231,** 1429–1431
41. Jones, S. A., Marchitto, K. S., Miller, J. N., and Norgard, M. V. (1984) *J. Exp. Med.* **160,** 1404–1420
42. Yang, Y., Janota, K., Tabei, K., Huang, N., Siegel, M. M., Lin, Y.-I., Rasmussen, B. A., and Shlaes, D. M. (2000) *J. Biol. Chem.* **275,** 26674–26682
43. Gardina, P. J., Bormans, A. F., Hawkins, M. A., Meeker, J. W., and Manson, M. D. (1997) *Mol. Microbiol.* **23,** 1181–1191
44. Norgard, M. V., Chamberlain, N. R., Swancutt, M. A., and Goldberg, M. S. (1986) *Infect. Immun.* **54,** 500–506
45. Zrein, M., Maure, I., Boursier, F., and Soufflet, L. (1995) *J. Clin. Microbiol.* **33,** 525–527
46. Hagedorn, H.-J., Kraminer-Hagedorn, A., De Bosschere, K., Hulstaert, F., Pottel, H., and Zrein, M. (2002) *J. Clin. Microbiol.* **40,** 973–978
47. Cox, D. L., Chang, P., McDowall, A., and Radolf, J. D. (1992) *Infect. Immun.* **60,** 1076–1083
48. Radolf, J. D., Chamberlain, N. R., Clausell, A., and Norgard, M. V. (1988) *Infect. Immun.* **56,** 490–498
49. Hayes, N. S., Muse, K. E., Collier, A. M., and Baseman, J. B. (1977) *Infect. Immun.* **17,** 174–186
50. Luthy, L., Grutter, M. G., and Mittl, P. R. E. (2002) *J. Biol. Chem.* **277,** 10187–10193
51. Esnouf, R. (1999) *Acta Crystallogr. Sect. D* **55**, 938–940
52. Nicholls, A., Sharp, K. A., and Honig, B. (1991) *Proteins* **11,** 281–296

[2] M. V. Norgard and M. S. Goldberg, unpublished data.